Acta Crystallographica Section D
Biological Crystallography
ISSN 0907-4449

Crystallization and preliminary X-ray study of the edema factor exotoxin adenylyl cyclase domain from *Bacillus anthracis* in the presence of its activator, calmodulin

Chester L. Drum,[a] Yuequan Shen,[b] Phoebe A. Rice,[c] Andrew Bohm[d]† and Wei-Jen Tang[a,b]*†

[a]Committee on Neurobiology, The University of Chicago, 924 East 57th Street, Chicago, IL 60637, USA, [b]Ben-May Institute for Cancer Research, The University of Chicago, 924 East 57th Street, Chicago, IL 60637, USA, [c]Department of Biochemistry and Molecular Biology, The University of Chicago, 924 East 57th Street, Chicago, IL 60637, USA, and [d]Boston Biomedical Research Institute and Tufts University School of Medicine, Boston, USA

† Collaborative principal investigators who contributed equally to this work.

Correspondence e-mail: wtang@midway.uchicago.edu

Received 10 July 2001
Accepted 4 September 2001

Edema factor from *Bacillus anthracis* is a 92 kDa secreted adenylyl cyclase exotoxin and is activated by the host-resident protein calmodulin. Calmodulin is a ubiquitous intracellular calcium sensor in eukaryotes and activates edema factor nearly 1000-fold upon binding. While calmodulin has many known effectors, including kinases, phosphodiesterases, motor proteins, channels and type 1 adenylyl cyclases, no structures of calmodulin in complex with a functional enzyme have been solved. The crystallization and initial experimental phasing of crystals containing a complex of edema factor adenylyl cyclase domain and calmodulin are reported here. The edema factor–calmodulin complex crystallizes in three different space groups. A native data set in the *I*222 space group has been collected to 2.7 Å and the self-rotation function solution suggests three edema factor–calmodulin complexes in each asymmetric unit. Initial 4 Å phases were obtained by selenomethionyl MAD in combination with two heavy-atom derivatives. These phases were successfully extended to 2.7 Å using NCS averaging.

1. Introduction

The mechanisms through which pathogenic bacteria cause illness are the result of significant communication and co-evolution between eukaryotic and prokaryotic cells. *B. anthracis*, the microbe that causes anthrax, defeats the host defense system by secreting three exotoxins (Dixon *et al.*, 1999). One of these exotoxins, edema factor (EF), is a calmodulin-activated adenylyl cyclase and can increase the level of intracellular cyclic AMP to a pathologic level, upsetting water homeostasis. EF is believed to be responsible for the massive edema and impaired neutrophil function seen in cutaneous anthrax. The N-terminal 250 amino-acid region of EF is required for EF to enter into the cytosol of host cells and the C-terminal 510 amino-acid region has calmodulin-activated adenylyl cyclase activity (Labruyere *et al.*, 1990; Drum *et al.*, 2000). Fluorescent resonance energy-transfer experiments using labeled calmodulin indicate that calmodulin binds EF in an extended conformation (Drum *et al.*, 2000) which is expected to be different from the canonical calmodulin–target interaction seen in previous crystal and NMR structures.

The structural characterization of the adenylyl cyclase domain of EF holds promise for insight in several different areas. Firstly, secreted adenylyl cyclases compose a multigene family of exotoxins produced by three distinct pathogenic bacteria, *B. anthracis* *Bordetella pertussis* and *Pseudomonas aeruginosa*. The structural features peculiar to this homologous family may provide insight into overall functional themes of toxin activation and inhibition. Secondly, the catalytic rate of EF is approximately 100 times faster than that of membrane-bound adenylyl cyclases, the catalytic core domain of which has been structurally determined (Tesmer *et al.*, 1997). With no sequence homology detectable between the two adenylyl cyclase families, a structural understanding of the active site of EF may yield a novel fold used for the cyclization of ATP or a variant on the di-metal mediated catalysis used by membrane-bound adenylyl cyclases (Tesmer *et al.*, 1999). Thirdly, the mechanism of activation with which the binding of calmodulin regulates the production of cyclic AMP may hold implications for inhibitory strategies of the toxin as well as structural themes applicable to other calmodulin-binding enzymes. In this paper, we describe the purification, crystallization and preliminary X-ray diffraction studies of the adenylyl cyclase domain of EF bound to calmodulin.

2. Materials and methods

2.1. Purification of H6-EF3, EF3-CH6 and calmodulin

The adenylyl cyclase domain of EF (290–800) was engineered with a hexahistidine tag on either its N- or C-terminus under the control of a prokaryotic Trc promoter, referred to as H6-EF3 and EF3-CH6, respectively. The

purification of EF3-CH6 and H6-EF3 (both pI = 8.9) was performed with modifications to that described in Drum *et al.* (2000). Briefly, crude *Escherichia coli* lysate was passed through a DEAE column to remove acidic *E. coli* proteins directly onto a Macro-S column. A salt gradient was then applied to the Macro-S column only and the peak fraction containing EF3 pooled. The enriched EF3 was loaded onto a nickel-chelating Sepharose column and eluted with 100 m*M* imidazole pH 7.0. The greater than 95% pure EF3 protein was then further purified with a Pharmacia Source-S column. The purity of the resultant edema factor was greater than 98% and was concentrated to greater than 40 mg ml^{-1}. The protein could be stored at 193 K in 10 m*M* Tris pH 7.5 buffer. Typical yields for a preparation of H6-EF3 and EF3-CH6 gave 80 and 45 mg, respectively, from a 12 l *E. coli* culture. Purification of calmodulin was carried out through induction of the expression plasmid pAED4-hCaM in *E. coli* BL21(DE3) cells as described in Drum *et al.* (2000).

2.2. Crystallization

All crystals of the EF3–calmodulin complex were grown by the hanging-drop method. The protein solution (2 µl) was mixed in a 1:1 ratio with the crystallization buffer and allowed to equilibrate *via* vapor diffusion over 500 µl of well solution at 277 K. Crystal Screens I and II (Hampton Research) were used to find crystallization conditions for edema factor in complex with calmodulin. Initially, a large proportion of the screened conditions produced a large precipitate upon mixing with the protein. In each case where this occurred, the condition was diluted in the well until precipitation was no longer observed in a newly set-up drop. Refinement of the initial condition resulted in single crystals that grew approximately 3–6 weeks (Table 1). Lanthanide and 3′-deoxy ATP (5 m*M*), a non-hydrolyzable ATP analog, both facilitated crystal seeding and growth. The washed crystals were analyzed by SDS–PAGE and mass spectrometry and appeared to contain EF3 and calmodulin in a 1:1 ratio. Although both H6-EF3 and EF3-CH6 could form crystals when mixed with calmodulin, the best diffraction and most regular crystallization kinetics were observed with EF3-CH6, the C-terminal hexahistidine-tagged protein, in combination with calmodulin. For heavy-metal derivatization, the crystals were soaked with saturated uranium fluoride for 30 min or 10 m*M* triethyl lead acetate for 2 h.

2.3. Cryoprotection

The approximately 0.4 × 0.4 × 0.6 mm crystals were transferred into an identical mother liquor containing 30% glycerol by slowly ramping from the initial glycerol concentration to 30% glycerol over a period of 10 h and allowing the crystal to soak in the 30% glycerol solution for greater than 12 h. The crystal was then frozen in liquid propane and data were collected at 100 K (Table 2). Although many surface fissures were observed on the crystal, X-ray analysis showed relatively low mosaicity and increased diffraction strength compared with similar crystals that were cryoprotected with faster exchange times.

2.4. Data collection and processing

For the data from EF3-CH6–selonomethionyl calmodulin, an EXAFS experiment was used to find the selenium *K* edge before data were collected at inflection-point, peak and remote wavelengths. Initially, the selenium edge was obscured by background fluorescence from the arsenic moiety of 100 m*M* cacodylic acid, included as the cryoprotectant buffer. However, narrowing of the bandpass of the fluorimeter to selectively amplify the selenium fluorescence allowed accurate tuning of the monochromator to the selenium edge. The native data was reduced with *MOSFLM* (Leslie, 1992), data from the uranium fluoride soak with *HKL* (Otwinowski & Minor, 1997), data with selenomethionyl calmodulin with *HKL*2000 (Otwinowski & Minor, 1997) and data from the triethyl lead acetate soak with *XDS* (Kabsch, 1993).

3. Results and discussion

Minor changes in crystallization conditions produced crystals of three distinct space groups, *I*222, $P3_121$ and $P2_12_12_1$ (Table 1). Crystals of space group *I*222 (Table 2) were used for the structure determination because they were the most reproducible and were less often twinned than the other space groups. The EF–calmodulin crystals with space group $P3_121$ have unit-cell parameters $a = b = 172.3$, $c = 196.8$ Å; the $P2_12_12_1$ crystals have unit-cell parameters $a = 183.5$, $b = 217.3$, $c = 322.9$ Å. The assumption of three edema factor–calmodulin complexes

Table 1
Crystallization conditions for the crystal forms of the EF–calmodulin complex.

	*I*222	$P3_121$	$P2_12_12_1$
EF3 (14.6 mg ml^{-1})	EF3-CH6	EF3-CH6	H6-EF3
Calmodulin (mg ml^{-1})	6.2	6.2	5.4
100 m*M* sodium cacodylate	pH 6.5	pH 6.0	pH 6.5
Ammonium sulfate (m*M*)	350	450	300
PEG 8000 (%)	10	10	10
Glycerol (%)	20	18	0
$MgCl_2$ (m*M*)	1	2	1
$YbCl_3$ (m*M*)	0.3	0.3	0

Table 2
Statistics of the native and derivatized EF–calmodulin complex data sets.

Values in parentheses are for the highest resolution shell. No cutoffs were applied to the data for this analysis.

Protein	Native EF3-CH6/ calmodulin	EF3-CH6/ Se-Met calmodulin	H6-EF3/ calmodulin (uranyl fluoride)	H6-EF3/ calmodulin (triethyl lead acetate)
Beamline	APS, 14-BM-C	APS, ID-19	NSLS, X4a	Rotating anode
Space group	*I*222	*I*222	*I*222	*I*222
Unit-cell parameters (Å)				
a	117.60	116.03	116.73	116.49
b	167.44	166.33	165.39	166.88
c	343.48	343.11	345.16	343.99
Total observations	875650†	261943	100399	118672
Unique observations	80665	29991	24117	33477
Resolution (Å)	2.75	3.8	4.0	4.0
R_{sym} (%)	9.7 (26.4)	7.6 (16.4)	11.0 (34.1)	11.0 (38.0)
$I/\sigma(I)$	4.6 (2.8)	14.0 (8.7)	4.3 (2.0)	11.3 (3.5)
Completeness(%)	91.6 (57.2)	90.1 (92.1)	80.0 (79.6)	96.6 (97.7)
Multiplicity	10.9 (3.3)	8.7 (6.1)	4.16 (4.2)	3.54 (3.3)
R_{merge}‡ (%)		29.0	43.7	28.9
Phasing power (acentrics)§				
Isomorphous		Peak, 2.18; inflection, 2.8	0.81	1.17
Anomalous		Peak, 1.39; inflection, 1.26	0.82	0.00
Cullis *R* (acentrics)§				
Isomorphous		Peak, 0.49; inflection, 0.43	0.96	0.90
Anomalous		Peak, 0.85; inflection, 0.88	0.85	0.00

† For the native data set, 120° of data was collected in 0.5° oscillations with two κ angles separated by 40°. Data were then collected with short exposures to compensate for the multiple overloads observed in the low-resolution reflections. ‡ R_{merge} statistics were generated using *SCALEIT* (Howell & Smith, 1992). § Calculated using *SHARP* (La Fortelle & Bricogne, 1997).

(228 kDa) in the $I222$ and $P3_121$ asymmetric units, yields a V_M of 3.6 and 4.0 Å^3 Da^{-1}, respectively (solvent content of ~65% and 70%). A similar V_M and solvent content (3.3 Å^3 Da^{-1} and 62%) predicts 12 EF3–calmodulin complexes in the $P2_12_12_1$ space group. The presence of several distinct space groups produced by similar crystal conditions suggested a relationship between crystallographic operators and predicted a threefold non-crystallographic symmetry operator parallel to the *bc* diagonal of the $I222$ space group. A self-rotation function search in the $I222$ space group reveals a significant peak in the $\kappa = 120^\circ$ section at the expected position, confirming the presence of a non-crystallographic threefold axis in the asymmetric unit (Fig. 1).

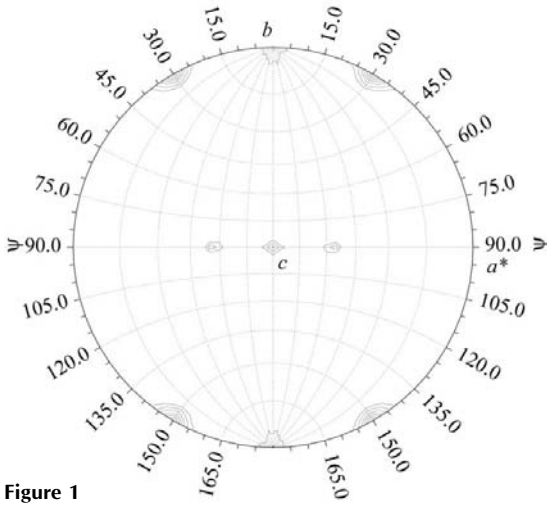

Figure 1
Self-rotation function with the $I222$ crystal form of the EF3–calmodulin complex using native data between 15.0 and 4.0 Å and a 30.0 Å radius of integration in the $\kappa = 120^\circ$ section. The plot was contoured starting at 15σ with an interval of 3σ. This figure was produced using *GLRF* (Tong & Rossmann, 1990).

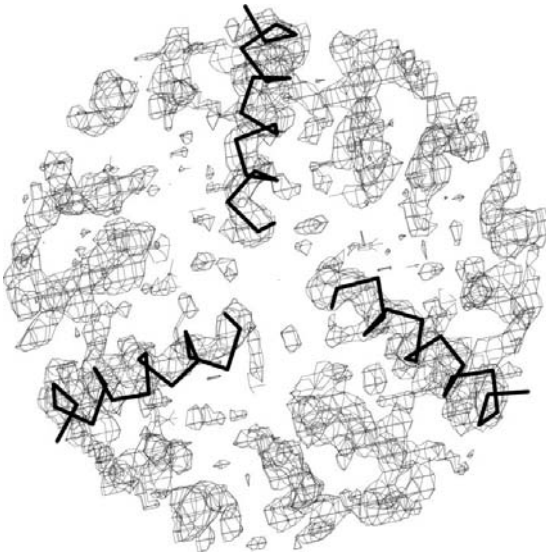

Figure 2
FOM-weighted F_o map calculated from solution of the combined phases from selenomethionine, uranium and lead. The helices from each of the three non-crystallagraphically related molecules in the asymmetric unit are shown. This figure was produced using *XTALVIEW* (McRee, 1992).

We grew crystals from the complex of EF3 and selenomethionyl calmodulin (Table 2). Calmodulin contains nine methionines, while EF3 has only three. Selenium incorporation was confirmed by the existance of a peak in the self-rotation function calculated using anomalous difference Patterson maps. This peak was in roughly the same position as that seen in the self-rotation function using only native data. After numerous unsuccessful attempts to interpret the anomalous and isomorphous difference Pattersons using *HASSP*, *RSPS* (Knight, 2000) and *SOLVE* (Terwilliger & Berendzen, 1999), a direct-methods algorithm, *Shake-n-Bake* (Weeks & Miller, 1999), was applied to the anomalous differences. Truncating the data at 4 Å and applying an $E/\sigma(E)$ cutoff of 1 allowed the successful location of eight of the expected 27 seleniums, resulting in a ratio of one resolvable selenium per 167 amino acids. Additional, potential sites located using difference Fourier maps were filtered based on the relative positions of the methionines within a previously solved calmodulin structure (Babu *et al.*, 1985) and the expected threefold symmetry within the asymmetric unit. After 12 selenium sites had been identified, the solvent flattened phases produced significant peaks in cross Fourier maps from data of crystals soaked with either uranium fluoride or triethyl lead acetate (Table 2), corresponding to five uranium and five lead sites. Using *SHARP* (La Fortelle & Bricogne, 1997), an experimental 4 Å map was calculated and solvent flattened with *DM* (Cowtan, 1994).

Owing to the poor quality of the initial experimental phases, map averaging was required to identify the remaining 22 heavy-atom sites. After skeletonization of the density in *MAPMAN* (Kleywegt & Jones, 1999), a mask was drawn around each monomer using *MAMA* (Kleywegt & Jones, 1999) and operators relating the three enzymes were refined with *IMP* (Kleywegt & Read, 1997). Maps were rotated and averaged using *MAPROT* (Stein *et al.*, 1994); *SIGMAA* (Read, 1986) was used to combine the back-transformed phases with the original experimental phases. The improved phases were used to find the remaining 15 Se, four U and three Pb sites in cross difference Fourier maps, resulting in an overall Figure of merit (FOM) of 0.63 for acentric reflections. A section from FOM-weighted F_o map without density modification is shown in Fig. 2. The resultant refined operators were used as starting points for eventual iterative averaging, solvent flattening and phase combination and extension from 4 to 2.75 Å using *DM* (Cowtan, 1994).

Although objective evaluation of experimental phases can be difficult, several factors point to the validity of experimental phasing. Unaveraged phases determined from the refinement of all 47 identified heavy-atom sites yielded an overall FOM of 0.63; phasing power and Cullis R statistics for each derivative are listed in Table 2. In the resulting map, electron density with clear secondary-structure features is visible and threefold symmetry is visible within the asymmetric unit (Fig. 2), unique from any expected crystallographic symmetry axis and consistent with the solution to the native self-rotation function. Model building is currently under way.

WJT was the recipient of an American Heart Associate Established Investigator Award. We are grateful to Drs Keith Moffat, Wilfried Schildkamp, Keith Brister, Gary Navrotski, Reinhard Pahl, Zhong Ren, Vukica Srajer, Tsu-Yi Tang and Jay Von Osinski at APS BioCars 14-BMC and 14-BMD, and Dr Duke at APS SBC 19-ID for their help in data collection, Dr Celia Harrison at Boston Biomedical Research Institute for making uranium fluoride and Dr Xiaojing Yang at Renz Research Inc. for the maintenance of computer hardware and software. This work was supported by National Institutes of Health grants GM53469, GM62548 and DA05778 (to CD).

References

Babu, Y. S., Sack, J. S., Greenhough, T. J., Bugg, C. E., Means, A. R. & Cook, W. J. (1985). *Nature (London)*, **315**, 37–40.
Cowtan, K. (1994). *Jnt CCP4/ESF–EACBM Newsle. Protein Crystallogr.* **31**, 34–38.
Dixon, T. C., Meselson, M., Guillemin, J. & Hanna, P. C. (1999). *N. Engl. J. Med.* **341**, 815–826.

Drum, C. L., Yan, S. Z., Sarac, R., Mabuchi, Y., Beckingham, K., Bohm, A., Grabarek, Z. & Tang, W. J. (2000). *J. Biol. Chem.* **275**, 36334–36340.
Howell, P. L. & Smith, G. D. (1992). *J. Appl. Cryst.* **25**, 81–86.
Kabsch, W. (1993). *J. Appl. Cryst.* **26**, 795–800.
Kleywegt, G. J. & Jones, T. A. (1999). *Acta Cryst.* D**55**, 941–944.
Kleywegt, G. J. & Read, R. J. (1997). *Structure*, **5**, 1557–1569.
Knight, S. D. (2000). *Acta Cryst.* D**56**, 42–47.
La Fortelle, E. de & Bricogne, G. (1997). *Methods Enzymol.* **276**, 472–494.
Labruyere, E., Mock, M., Ladant, D., Michelson, S., Gilles, A. M., Laoide, B. & Barzu, O. (1990). *Biochemistry*, **29**, 4922–4928.
Leslie, A. G. W. (1992). *Jnt CCP4/ESF–EAMCB Newsl. Protein Crystallogr.* **26**.
McRee, D. E. (1992). *J. Mol. Graph.* 10, 44–46.
Otwinowski, Z. & Minor, W. (1997). *Methods Enzymol.* **276**, 307–326.
Read, R. J. (1986). *Acta Cryst.* A**42**, 140–149.
Stein, P. E., Boodhoo, A., Armstrong, G. D., Cockle, S. A., Klein, M. H. & Read, R. J. (1994). *Structure*, **2**, 45–57.
Terwilliger, T. C. & Berendzen, J. (1999). *Acta Cryst.* D**55**, 849–861.
Tesmer, J. J., Sunahara, R. K., Gilman, A. G. & Sprang, S. R. (1997). *Science*, **278**, 1907–1916.
Tesmer, J. J., Sunahara, R. K., Johnson, R. A., Gosselin, G., Gilman, A. G. & Sprang, S. R. (1999). *Science*, **285**, 756–760.
Tong, L. & Rossmann, M. G. (1990). *Acta Cryst.* A**46**, 783–792.
Weeks, C. M. & Miller, R. (1999). *J. Appl. Cryst.* **32**, 120–124.